Deep Learning for Pulse Repetition Interval Classification

Ha P. K. Nguyen, Ha Q. Nguyen and Dat T. Ngo
Viettel Research and Development Institute, Hoa Lac High-tech Park, Hanoi, Vietnam

Keywords: Pulse Repetition Intervals, PRI Modulation Classification, Convolutional Neural Network, Deep Learning.

Abstract: Pulse Repetition Intervals (PRI)—the distances between consecutive times of arrival of radar pulses—is an important characteristic of the radar emitting source. The recognition of various PRI modulation types is therefore a key task of an Electronic Support Measure (ESM) system for accurate identification of threat emitters. This problem is challenging due to the missing and spurious pulses. In this paper, we introduce a deep-learning-based method for the classification of 7 popular PRI modulation types. In this approach, a convolutional neural network (CNN) is proposed as the classifier. Our method works well with raw input PRI sequences and, thus, gets rid of all preprocessing steps such as noise mitigation, feature extraction, and threshold setting, as required in previous approaches. Extensive simulations demonstrate that the proposed scheme outperforms existing methods by a significant margin over a variety of PRI parameters, especially in severely noisy conditions.

1 INTRODUCTION

An Electronic Support Measures (ESM) system captures radar signals from multiple sources and identifies the radars based on several characteristics of the received signals. One of the most important features of a radar signal is the sequence of pulse repetition intervals (PRI) that consists of distances between the times of arrival (TOAs) of consecutive radar pulses. In modern radar technology, various types of complicated PRI modulation are used rather than just a simple constant pattern. Therefore, the recognition of PRI modulations will greatly help identify the emitting sources. This is, however, far from a trivial problem due to the unavoidable miss-detections and false alarms of the TOAs, which might result in very noisy PRI sequences. In addition, the diversity of parameters in each type of PRI modulation makes the recognition task much more challenging.

To solve the PRI modulation classification issue, extensive research has been conducted. Existing methods can generally be divided into 3 categories: statistics-based, decision-tree-based, and learning-based. In the classical statistics-based methods (Mardia, 1989; Milojevic and Popovic, 1992), histogram techniques are used to recognize PRI modulation types. Since these methods are simple, they work only with a limited number of PRI modulation types and their performances are drastically degraded in noisy situations. Decision-tree based methods (Kauppi and Martikainen, 2007; Hu and Liu, 2010; Song et al., 2010) usually consist of three steps: first, a noise mitigation technique is applied to compensate the impact of missing and spurious pulses on the PRI sequence; second, discriminative features are extracted from the denoised PRI sequence; and, finally, a decision-tree is carried out to differentiate PRI modulation types. The main shortcoming of decision-tree-based approaches is the requirement of heavily-handcrafted thresholds, which are not only time-consuming but also very sensitive to the level of noise and the change of PRI parameters. Existing learning-based methods for PRI modulation classification often rely on *shallow* neural networks. Noone proposed in (Noone, 1999) a neural-network classifier with a single hidden layer that is trained on a set of the second differences of the TOAs. More recently, Liu and Zhang introduced in (Liu and Zhang, 2017) a feed-forward neural network consisting of an input layer with 3 features derived from (Noone, 1999) and a single hidden layer of only 8 neurons. This method can only classify 4 types of PRI modulations. It is noteworthy that all the aforementioned learning-based methods require a careful design of features and a feature extraction process before the neural network can be applied. This drawback prevents these methods from quick adaptation to changes in the PRI modulations.

Recently, deep learning (LeCun et al., 2015; Goodfellow et al., 2016) has emerged as a powerful tool for many classification tasks. In this paper,

Nguyen, H., Nguyen, H. and Ngo, D.
Deep Learning for Pulse Repetition Interval Classification.
DOI: 10.5220/0007253203130319
In *Proceedings of the 8th International Conference on Pattern Recognition Applications and Methods (ICPRAM 2019)*, pages 313-319
ISBN: 978-989-758-351-3

we introduce a novel deep-learning-based scheme in which a deep Convolutional Neural Network (CNN) is trained to classify 7 types of PRI modulations. To the best of our knowledge, we are the first to adopt a deep learning approach to solve this problem. The main advantage of the proposed method is that the CNN takes raw PRI sequences as input and, therefore, bypasses the feature extraction procedures as in previous approaches. Furthermore, as will be demonstrated in simulations, our approach is very noise-robust and effective for classifying PRI modulations compared to existing methods. In particular, for a wide range of missing and spurious pulse fractions, the proposed method noticeably outperforms the other competitors with an accuracy gap of at least 2%. This gap even increases quickly with the noise level.

The rest of this paper is organized as follows: Section 2 presents some preliminaries about PRI modulations; Section 3 describes the architecture of the CNN; Section 4 evaluates the performance of the proposed method on simulated data against state-of-the-art classifiers; and, finally, Section 5 concludes the paper.

2 PRI MODULATIONS

An ESM system receives radar signals and estimates the parameters associated with each of the detected pulses. Given a sequence of TOAs of the radar signal $\{t[n]\}_{n=0}^{N}$, where $t[n]$ is the estimated arrival time of the nth radar pulse and N is the number of detected pulses, the PRI sequence is defined as

$$p[n] = t[n+1] - t[n], \quad n = 0, \ldots, N-1. \tag{1}$$

The pattern of a PRI sequence is dictated by a specific PRI modulation type. In this paper, we consider the following 7 PRI modulation types that are frequently used in modern radar systems:

1. Constant (CST): the simplest PRI modulation in which the pulses are equally spaced.
2. Sliding Up (SLU): the PRIs periodically linearly increase with respect to some slope.
3. Sliding Down (SLD): the PRIs periodically linearly decrease with respect to some slope.
4. Jittered (JIT): the PRIs are randomized according to a Gaussian distribution.
5. Staggered (STG): the PRIs periodically jump through a fixed number of levels.
6. Dwell & Switch (DS): piecewise-constant PRIs, where each piece is called a burst.

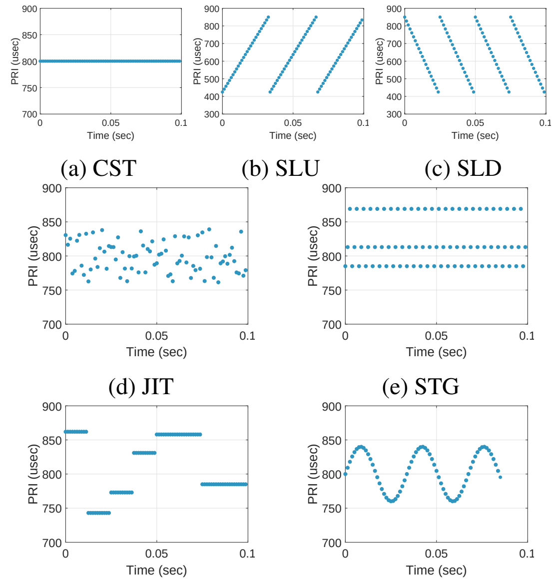

(a) CST (b) SLU (c) SLD (d) JIT (e) STG (f) DS (g) WOB

Figure 1: Ideal examples of the 7 PRI modulations.

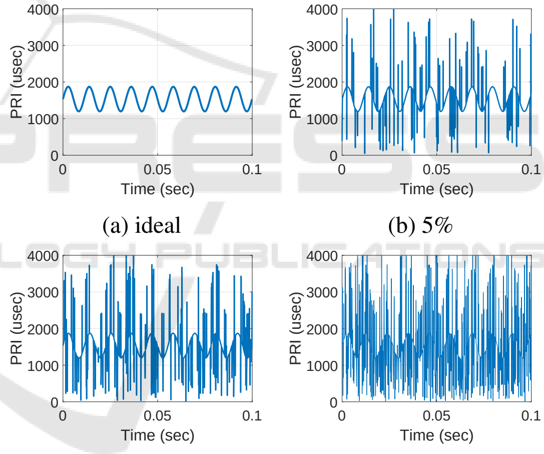

(a) ideal (b) 5% (c) 10% (d) 30%

Figure 2: A Wobulated PRI sequence with different fractions of missing and spurious pulses. Each subplot from (b) to (d) is captioned with the rate of missing and spurious pulses.

7. Wobulated (WOB): sinusoidal PRIs.

Fig. 1 illustrates ideal examples of these PRI modulations. In practice, however, PRIs are subject to perturbations, miss-detections (missing pulses) and false alarms (spurious pulses) due to the imperfection of the TOA estimation process. The combined effect of these errors may significantly distort the original form of a PRI sequence, as showed in Fig. 2, posing a great challenge for the classification task. A common method for suppressing the speckle noise on PRI sequences is to apply median filters as a preprocessing step. However, the choice of the filter length, which is critical, is very sensitive to the noise level. Furthermore, the median filtering might destroy the pattern of the PRIs, making the classification even harder in some cases. Also, note that existing classification methods rely on handcrafted features and/or thresholds are that are not robust to a wide range of noise imposed on PRI sequences. The above shortcomings can be overcome with a deep Convolutional Neural Network (CNN) as will be described next.

3 CNN ARCHITECTURE

We propose in this section a CNN, whose architecture is depicted in Fig. 3, for the PRI classification. As opposed to the previous neural-network schemes, the input to the proposed CNN is the *raw* PRI sequence of fixed size 1×1000, supposedly obtained from a TOA estimation algorithm. That is, both the denoising and the feature extraction are handled by the network itself. This is done via a concatenation of 8 convolution layers and 2 fully connected (dense) layers. Roughly speaking, the convolution layers play the role of a feature extraction that is robust to noise, while the dense layers take care of the classification based on the output of the final convolution layer. The whole network is trained end-to-end on a dataset of PRI sequences labeled with ground-truth modulation types indexed from 0 to 6. Note that before feeding a PRI sequence $p[n]$ to the network, we normalize it as

$$p_{\text{norm}}[n] = \frac{p[n]}{\max_i p[i]}, \quad \forall n. \tag{2}$$

Following the design philosophy of the VGG-net (Simonyan and Zisserman, 2015), all filters used in the 8 convolution layers are of fixed size 1×3, resulting in a receptive field of $8 \times 2 + 1 = 17$ samples. The number of filters is decreased from 32 to 4 along the convolution layers. Note that, in each convolution layer, a *batch normalization* is used to combat the internal covariate shift as suggested in (Ioffe and Szegedy, 2015). Moreover, the Rectified Linear Unit (ReLU) is used as the activation function for all convolution layers. The result of the final convolution layer is 4 feature maps, each of size 1×1000, which are then flattened into a single feature vector of length 4000. This vector is fully connected to a layer of 256 neurons with ReLU activation. To prevent over-fitting, a dropout layer (Srivastava et al., 2014) with dropping ratio of 0.7 is inserted in between these layers. Finally, the output of the Dense-256 layer is transformed to a score vector of length 7 via the last fully connected layer with the softmax activation function. The score vector can be thought of as a probability distribution of the 7 classes.

The network weights are trained by minimizing a loss function defined as the cross-entropy between the output vector of the network and the one-hot vector associated with the ground-truth label of the input PRI sequence. This optimization procedure can be realized by a stochastic gradient descent algorithm. In the testing phase, the class of an input PRI sequence is simply determined by taking the index of the output vector that yields the maximum score.

4 PERFORMANCE EVALUATION

In order to evaluate the performance of our CNN-based PRI classification, a set of 140,000 randomly generated PRI sequences (20,000 for each modulation type) was used for training and another set of 35,000 (5,000 for each class) was used for testing. Both training and testing data were generated randomly according to a variety of parameters given in Table 1. It should be noted that the training set and the testing set are separated and different from each other. Therefore, the testing set can be fairly used to verify the accuracy and generalization of the proposed model. The data generation was performed in Matlab, while the training was implemented in Python with Keras library and TensorFlow backend, running on an Nvidia Tesla P100 GPU. The final CNN model was obtained after being trained for 100 epochs with Adam optimizer and with a learning rate of 10^{-4}.

We compare CNN with 3 state-of-the-art competitors including both decision-tree-based and learning-based methods as follows:

- The proposed scheme in (Song et al., 2010): This method is able to classify only 5 PRI modulation types (DS, SLD, SLU, JIT, and WOB) by applying a decision tree on features extracted from the symbolizations of PRI and differential PRI sequences. Hence, we refer to this method as Symbolization-based Decision Tree (**SDT**). The thresholds used in this algorithm were carefully chosen to optimize the classification accuracy.
- The proposed scheme in (Noone, 1999), which we call Transform-based Neural Network (**TNN**): This learning-based method uses the second differences of TOAs feature as the input of a feed-forward neural-network.
- The proposed scheme in (Liu and Zhang, 2017): This method uses a feed forward neural network consisting of an input layer with 3 extracted features based on the second differences of TOAs to classify 4 PRI modulation types (WOB, JIT, DS, and Sliding). It should be noted that in that pa-

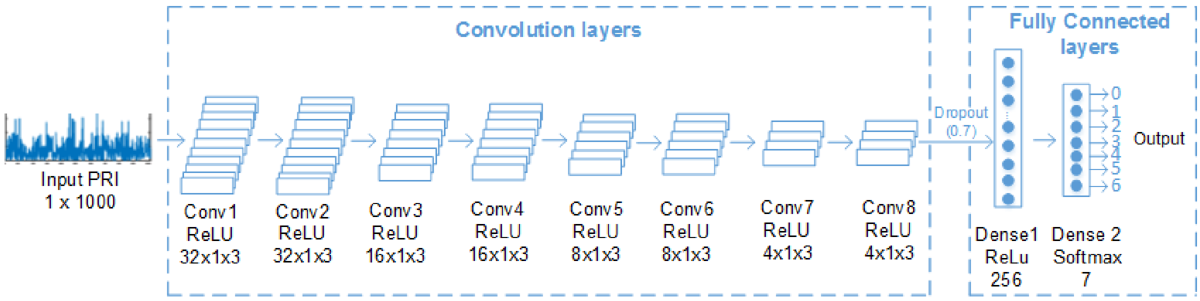

Figure 3: Architecture of the proposed CNN for PRI classification.

Table 1: PRI parameters used in simulations. Each PRI sequence is generated by a combination of parameters randomly selected from the given ranges.

Type	Parameters
All	Number of TOAs $= 1001$ PRI pertubation $= \pm(0.5 \div 2.0)\mu s$ Rate of Missing pulses $= (0 \div 30)\%$ Rate of Spurious pulses $= (0 \div 30)\%$
CST	PRI value $= (50 \div 4000)\mu s$
STG	PRI value $= (50 \div 4000)\mu s$ Number of PRI levels $= (2 \div 10)$
JIT	PRI value $= (50 \div 4000)\mu s$ PRI deviation $= (5 \div 20)\%$ of PRI value
DS	PRI value $= (50 \div 4000)\mu s$ Number of bursts $= (2 \div 10)$ Burst length $= (30 \div 120)$ pulses
Sliding	$\mathrm{PRI}_{\mathrm{max}}/\mathrm{PRI}_{\mathrm{min}}$ ratio $= (2 \div 6)$ $\mathrm{PRI}_{\mathrm{max}} \in \{200, 600, 1000, 1500, 2000, 4000\}$ Number of slides $= (2 \div 10)$
WOB	PRI mean value $= (50 \div 2000)\mu s$ $\mathrm{PRI}_{\mathrm{max}}/\mathrm{PRI}_{\mathrm{mean}}$ ratio $= (1.02 \div 1.5)$ Number of periods $= (2 \div 10)$

per, the authors combined two PRI modulations, SLU and SLD, into a single type called Sliding (SL). We name this scheme Improved Feed-forward Neural Network (**IFNN**).

Since TNN and IFNN are also learning-based, for a fair comparison, they were trained on the same training dataset of CNN. The training of these two networks was done in Matlab with Neural Network Toolbox. After training all the models, we used the same testing dataset to verify the PRI classification accuracy of CNN, TNN, IFNN, and SDT. The comparison of the 4 methods was performed on a mixed dataset of all noise levels, as well as on several datasets of specific noise levels.

4.1 Overall Accuracy

Figs. 4, 5, and 6 show the training and testing confusion matrices of CNN, TNN, and IFNN, respectively. Since SDT is a decision-based method without any training, we only report the confusion matrix of the testing dataset for this scheme in Fig. 7. It can be seen from Fig. 4 that the proposed CNN achieves a classification accuracy of 99.40% and 98.42% on the training dataset and testing dataset, respectively. It means that the recognition correctness of CNN is 24.42% higher than that of a typical decision-tree-based scheme, SDT. CNN also yields a superior performance compared to TNN, which only reaches a classification accuracy of 63.35% on the testing dataset. Additionally, comparing to a recent learning-based method, IFNN, CNN also improves the classification performance by about 2%. It is worth noting that our proposed scheme outperforms SDT and IFNN, although it should classify for many more PRI modulation classes. Moreover, by using only the raw noisy PRI sequences as input, our method can get rid of the threshold setting process of SDT and the preprocessing steps, such as noise compensation and feature extraction, of TNN and IFNN.

4.2 Accuracy with Varying Noise

In this subsection, we further investigate the effect of missing pulse rate and spurious pulse rate on the classification performance. We tested our CNN method against the other competitors under various noisy conditions by using different datasets with varying ranges of missing pulse rate and spurious pulse rate as follows:

- Dataset 1: Rates of missing and spurious pulses are randomly varied from 0% to 5%;
- Dataset 2: Rates of missing and spurious pulses are randomly varied from 5% to 10%;
- Dataset 3: Rates of missing and spurious pulses are randomly varied from 10% to 15%;
- Dataset 4: Rates of missing and spurious pulses are randomly varied from 15% to 20%;
- Dataset 5: Rates of missing and spurious pulses are randomly varied from 20% to 25%;

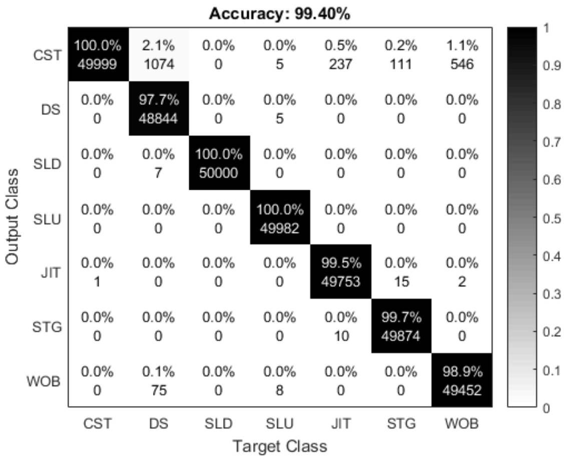

(a) Training

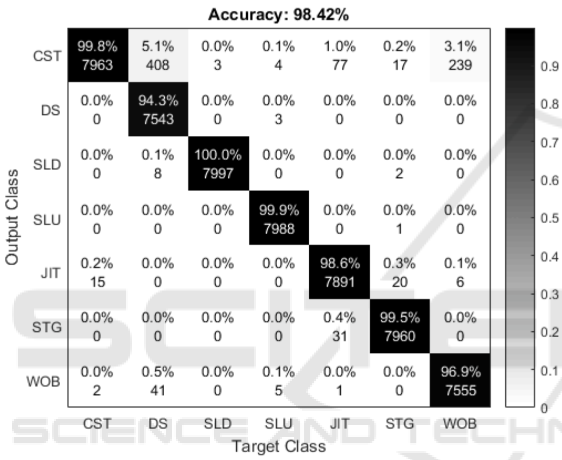

(b) Testing

Figure 4: Confusion matrices of CNN on the whole testing dataset with the rates of missing and spurious pulses ranging from 0% to 30%.

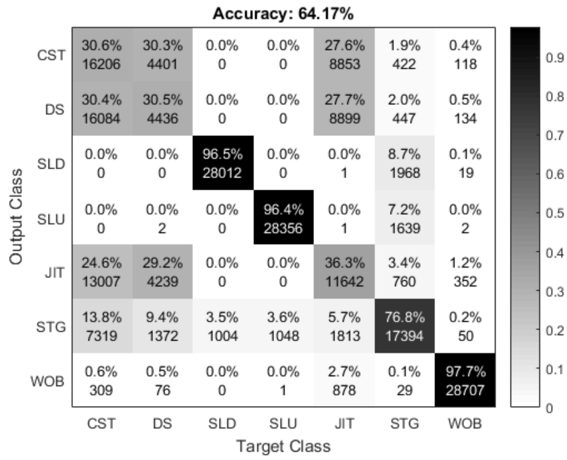

(a) Training

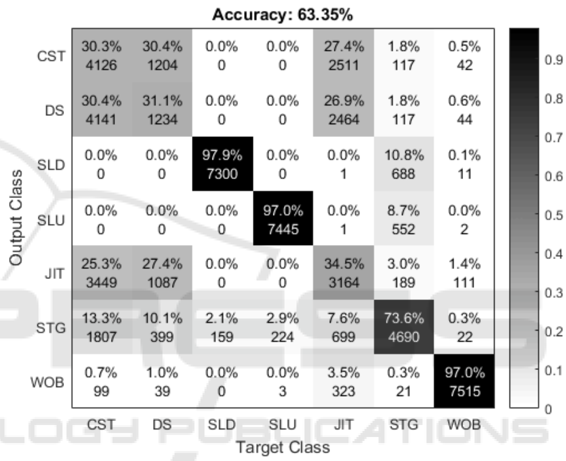

(b) Testing

Figure 5: Confusion matrices of TNN on the whole testing dataset with the rates of missing and spurious pulses ranging from 0% to 30%.

- Dataset 6: Rates of missing and spurious pulses are randomly varied from 25% to 30%.

Each of the above dataset contains 3000 samples for each PRI modulation type and is generated randomly with parameters presented in Table 1. Fig. 8 compares the classification accuracies of the 4 methods with varying ranges of missing and spurious pulse rate. It can be observed that TNN achieves the worst performance. The reason is that the second difference of PRI sequence is not adequate to discriminate many complex PRI modulation types. This feature is also very sensitive with missing and spurious pulses. In less noisy conditions, SDT performs quite well with an accuracy greater than 90%. However, its quality is seriously degraded when the missing and spurious pulse rates increase. Specifically, the accuracy of SDT is reduced by more than 40% when the fractions of missing and spurious pulse exceed 20%. This observation proves that the fixed thresholding of decision-tree-based methods is very vulnerable to noise and, thus, fails to classify the PRI modulations over a large range of miss-detections and false alarms.

It is remarkable that CNN and IFNN significantly outperform SDT and TNN. When the missing and spurious pulse rates are less than 20%, the classification accuracy of CNN and IFNN are 99.1% and 97.5% on average, respectively. Nevertheless, the performance gap between CNN and IFNN increases considerably with the rates of missing and spurious pulses. For instance, CNN attains an improvement of 6% compared to IFNN when the missing and spurious pulse rates are in the range from 25% to 30%. Again, we recall that CNN outperforms IFNN with many more classified PRI modulation types (7 of CNN against 4 of IFNN).

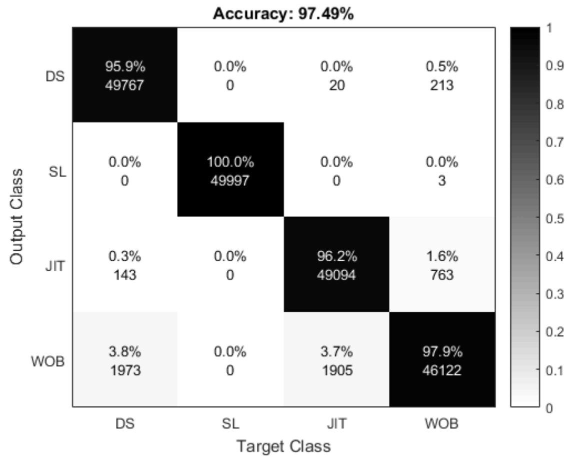

(a) Training

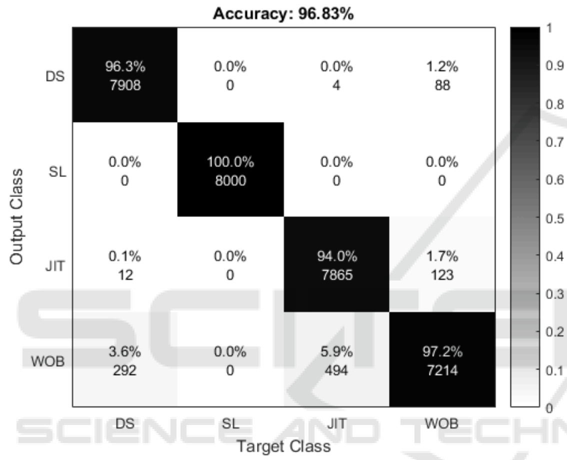

(b) Testing

Figure 6: Confusion matrices of IFNN on the whole testing dataset with the rates of missing and spurious pulses ranging from 0% to 30%.

From the above analysis, we can conclude that our CNN classifier is able to recognize different PRI modulation types with high accuracy and is resilient to heavily missing and spurious pulses.

5 CONCLUSION

In this paper, we have proposed a deep-learning-based method to solve the PRI modulation classification for the first time. We have trained a convolution neural network that can efficiently recognize 7 PRI modulation types. The major advantage of the proposed method is twofold. First, the input of our classifier is raw PRI sequences; thus, it can bypass the noise filtering and the tedious calibration of many thresholds in decision-tree-based methods, as well as the feature extraction in previous learning-

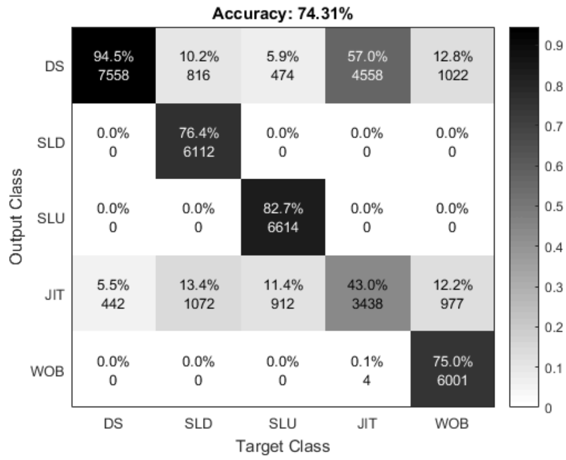

Figure 7: Confusion matrices of SDT on the whole testing dataset with the rates of missing and spurious pulses ranging from 0% to 30%. Training is not needed for this method.

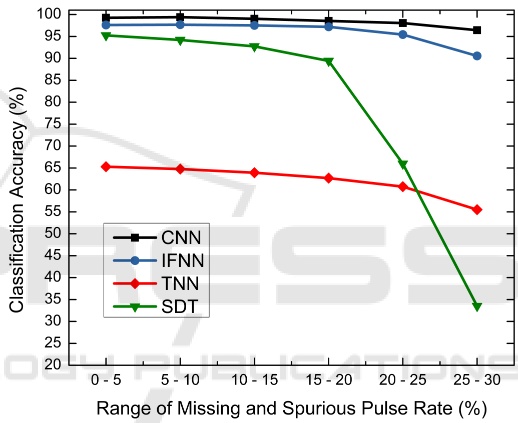

Figure 8: Classification accuracies of the 4 different methods are plotted against the range of missing and spurious rate.

based approaches. Second, in severely noisy environments with high missing and spurious pulse rates, our scheme still achieves an impressive classification accuracy, in contrast to other methods. The simulation results have demonstrated that our proposed method strikingly surpasses the state-of-the-art PRI classifiers on a wide range of simulation parameters. For future research, it is worth investigating deep neural networks for estimating the parameters associated to each type of PRI modulation after the classification.

REFERENCES

Goodfellow, I., Bengio, Y., and Courville, A. (2016). *Deep Learning*. MIT Press.

Hu, G. and Liu, Y. (2010). An efficient method of pulse repetition interval modulation recognition. In *Proc. IEEE*

Int. Conf. Commun. Mobile Comput., pages 287–295, Shenzhen, China.

Ioffe, S. and Szegedy, C. (Jul. 06-11, 2015). Batch normalization: Accelerating deep network training by reducing internal covariate shift. In *Proc. Int. Conf. Machine Learning (ICML)*, pages 1097–1105, Lille, France.

Kauppi, J.-P. and Martikainen, K. S. (2007). An efficient set of features for pulse repetition interval modulation recognition. In *Proc. IET Int. Conf. Radar Syst.*, pages 1–5, Edinburgh, UK.

LeCun, Y., Bengio, Y., and Hinton, G. (2015). Deep learning. *Nature*, 521:436–444.

Liu, Y. and Zhang, Q. (2017). An improved algorithm for PRI modulation recognition. In *Proc. IEEE Int. Conf. Signal Process. Commun. Comput.*, pages 1–5, Xiamen, China.

Mardia, H. K. (1989). New techniques for the deinterleaving of repetitive sequences. *IEE Proc. F Commun. Radar & Signal Process.*, 136(4):149–154.

Milojevic, D. J. and Popovic, B. M. (1992). Improved algorithm for the deinterleaving of radar pulses. *IEE Proc. F Commun. Radar & Signal Process.*, 139(1):98–104.

Noone, G. P. (1999). A neural approach to automatic pulse repetition interval modulation recognition. In *Proc. IEEE Information, Decision and Control (IDC)*, pages 213–218, Phoenix, AZ, USA.

Simonyan, K. and Zisserman, A. (2015). Very deep convolutional networks for large-scale image recognition. In *Proc. Int. Conf. Learning Representations (ICLR)*, pages 1–14, San Diego, USA.

Song, K. H., Lee, D. W., Han, J. W., and Park, B. K. (2010). Pulse repetition interval modulation recognition using symbolization. In *Proc. IEEE Int. Conf. Digit. Image Comput.: Techniques and Applications (DICTA)*, pages 540–545, Sydney, NSW, Australia.

Srivastava, N., Hinton, G., Krizhevsky, A., Sutskever, I., and Salakhutdinov, R. (2014). Dropout: A simple way to prevent neural networks from overfitting. *J. Machine Learning Research*, 15(1):1929–1958.